Saddle solitons: A balance between bi-diffraction and hybrid nonlinearity

6 authors, including:

Yi Hu
105 PUBLICATIONS **1,436** CITATIONS

SEE PROFILE

Cibo Lou
Nankai University
71 PUBLICATIONS **803** CITATIONS

SEE PROFILE

Peng Zhang
Changsha University of Science and Technology
30 PUBLICATIONS **933** CITATIONS

SEE PROFILE

Jingjun Xu
Nankai University
797 PUBLICATIONS **6,931** CITATIONS

SEE PROFILE

Some of the authors of this publication are also working on these related projects:

Terahertz phonon polariton and its applications: Terahertz integrated chip for sensing, time domain spectroscopy, future communication; and spatiotemporal super-resolution imaging View project

Weak Light Nonlinear Optics View project

Saddle solitons: a balance between bi-diffraction and hybrid nonlinearity

Yi Hu,[1] Cibo Lou,[1] Peng Zhang,[2] Jingjun Xu,[1] Jianke Yang,[3] and Zhigang Chen[1,2,*]

[1]*The Key Laboratory of Weak-Light Nonlinear Photonics, Ministry of Education and TEDA Applied Physics School, Nankai University, Tianjin 300457, China*
[2]*Department of Physics and Astronomy, San Francisco State University, San Francisco, California 94132, USA*
[3]*Department of Mathematics and Statistics, University of Vermont, Burlington, Vermont 05401, USA*
*Corresponding author: zhigang@sfsu.edu

We demonstrate self-trapping of light by simultaneously compensating normal and anomalous (saddle-shaped) diffractions with self-focusing and self-defocusing hybrid nonlinearity in optically induced ionic-type photonic lattices. Innovative two-dimensional gap solitons, named "saddle solitons," are established, whose phase and spectrum characteristics are different from all previously observed spatial solitons. © 2009 Optical Society of America

OCIS codes: 190.6135, 190.5330, 350.4238.

Despite the discovery of a variety of soliton entities in discrete systems [1], to our knowledge, it has not been possible to demonstrate a two-dimensional (2D) spatial soliton in a physical arrangement where an optical beam exhibits simultaneously normal and anomalous diffractions in different transverse directions. First, natural materials typically are not endowed with a *saddle-shaped* bi-diffractive property; second, it remains a challenge to find a nonlinear material that can support *hybrid* self-focusing and self-defocusing nonlinearities without changing experimental conditions. Previous work on nonlinear X waves and light bullets was aimed toward balancing of beam diffraction and pulse dispersion simultaneously, but in spatial domain alone compensation of normal and anomalous diffractions in the same experimental setting has not been realized.

Man-made periodic structures have shown many intriguing optical properties. In an optically induced 2D square lattice [2–4], for example, the high-symmetry X point in the first Bloch band is akin to a saddle point in diffraction spectrum [see Fig. 1(c)], where normal and anomalous diffractions coexist along orthogonal directions [5]. At this X point, a quasi-1D soliton train can be excited provided that an appropriate type of nonlinearity is used to balance beam diffraction in one particular direction, whereas in the orthogonal direction it is an extended plane wave [6]. The propagation constant of such a 1D soliton train could reside within the first Bloch band, thus named "in-band" or "embedded" solitons [7]. However, to simultaneously balance normal and anomalous diffractions for self-trapping of a 2D-localized optical beam, one needs orientation-dependent hybrid nonlinearity. Fortunately, such nonlinearity was found in our recent work with photorefractive nonlinear crystals under nonconventional bias (NCB) condition [8–10], in which coexistence of self-focusing and self-defocusing nonlinearities at two orthogonal directions has led to observation of controlled 1D soliton transition from different band edges or subband edges.

In this Letter, we employ the hybrid nonlinearity to demonstrate a type of spatial gap solitons, namely, "saddle solitons," by balancing the saddle-shaped diffraction in an optically induced 2D ionic-type lattice [10]. Such solitons have propagation constant residing in the Bragg reflection gap, but they differ from all previously observed solitons supported by a single self-focusing or self-defocusing nonlinearity. In addition, quasi-localized 2D in-band solitons are also identified, but they are not stable during propagation. Our theoretical analysis finds good agreement with experimental observations.

First, let us determine numerical solutions for the aforementioned saddle solitons from our theoretical model. In our NCB condition, the bias electric field is perpendicular to the crystalline c axis of a photorefractive strontium barium niobate (SBN) crystal
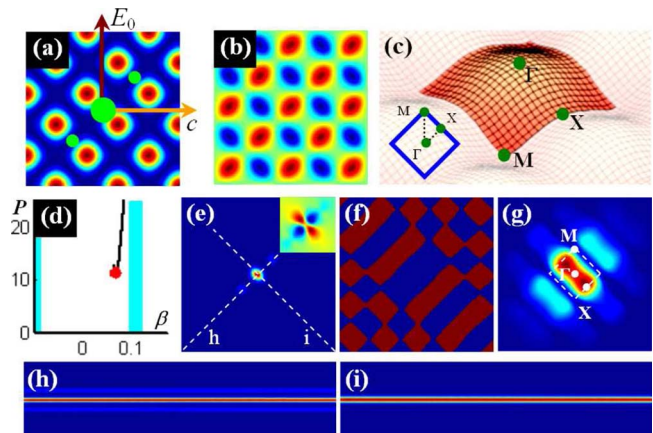

Fig. 1.　(Color online) (a) Orientations of crystalline c axis, bias field, and square lattice-inducing beam; (b) refractive index distribution of the induced ionic-type lattice; (c) extended first Bloch band; (d) Existence curve of saddle solitons at $V_0 = 0.94$; (e)–(g) Intensity pattern (associated index change shown in insert), phase structure, and Fourier spectrum of the saddle soliton at the marked point in (d); (h), (i) evolution of intensity profiles along dashed lines in (e) for 10 cm propagation of the soliton solution. Added squares in (c) and (g) mark the boundary of the first Brillouin zone.

[Fig. 1(a)] as used in our experiment. This arrangement gives rise to hybrid nonlinearity with the strongest self-focusing and self-defocusing effects along the two orthogonal directions [8,9]. In addition, the 2D square intensity pattern of the lattice-inducing beam shown in Fig. 1(a) creates a 2D ionic-type index lattice of Fig. 1(b) [10]. Light propagation in such a lattice under the NCB condition can be described by the following normalized equation [8]:

$$\left(\frac{\partial}{\partial z} - \frac{i}{2}\nabla^2\right)B(\vec{r}) = i\gamma\frac{\partial\varphi}{\partial x}B(\vec{r}), \tag{1a}$$

$$\nabla^2\varphi + \nabla\varphi\cdot\nabla\ln(1+I) = \frac{\partial}{\partial y}\ln(1+I), \tag{1b}$$

where $\nabla = \hat{x}(\partial/\partial x) + \hat{y}(\partial/\partial y)$, $B(\vec{r})$ is the amplitude of the probe beam, φ is the light-induced electrostatic potential, $\gamma = (k_0 l_0 n_0^2)^2 \gamma_{33} E_0/2$ is a normalized nonlinear parameter related to the electro-optic coefficient γ_{33} and the bias field E_0, k_0 is the wavenumber in vacuum, l_0 is an arbitrary length unit for scaling, and n_0 is the unperturbed refractive index of the crystal. The normalized total intensity is defined as $I = |B(\vec{r})|^2 + V(x,y)$, where $V(x,y) = V_0 \cos^2[\pi(x+y)/\sqrt{2}\Lambda]\sin^2[\pi(x-y)/\sqrt{2}\Lambda]$ is the intensity of the lattice-inducing beam with a spatial period Λ and peak intensity V_0. If we assume that the soliton solutions of Eq. (1) take the form $B(x,y,z) = b(x,y)\exp(i\beta z)$, with β being the propagation constant, then the envelope function $b(x,y)$ satisfies the following equation:

$$\left(\beta - \frac{1}{2}\nabla^2\right)b(x,y) = \gamma\frac{\partial\varphi}{\partial x}b(x,y). \tag{2}$$

By solving Eqs. (1) and (2), we obtain saddle soliton solutions residing in the first Bragg reflection gap as shown in Figs. 1(d) and 1(e), where the parameters used are $\gamma = 2$, $\Lambda = 8.6$, $V_0 = 0.94$. The phase structure and spectrum of the gap solitons established here are different from those of 2D gap solitons found before. Specifically, the phase structure of the central soliton region [Fig. 1(f)] fits that of the Bloch modes from X points, and the power spectrum [Fig. 1(g)] also concentrates mostly at the two X points within the first Brillouin zone (BZ). This indicates that the saddle solitons must consist of modes from the interior X points of the first band, although far away from the soliton center staggered phase characteristic to band edge M point modes is evident. These 2D saddle solitons differ from previously observed quasi-1D embedded or gap solitons (also from first-band X points), which are localized only in one direction [6,9], and from the reduced symmetry solitons created solely by self-focusing nonlinearity (but from second-band X points) [11]. Their stable long-distance propagation [Figs. 1(h) and 1(i)] obtained from simulation with numerical solutions of Fig. 1(e) as the initial condition suggests that such saddle solitons could be observed in experiment.

Our experimental arrangement is similar to that used in our earlier work [6,9]. A laser beam at a wavelength of 532 nm splits into two parts with a polarizing beam splitter. The ordinarily polarized part (lattice-inducing beam) passes through a rotating diffuser and an amplitude mask, and is then imaged onto a SBN:60 crystal to construct a 2D ionic-type photonic lattice (about 26 μm spacing). The relative orientation between the c axis, bias field, and the lattice beam is as depicted in Fig. 1(a). The e-polarized part splits again into two beams: one of them is focused at the crystal input as a probe beam to generate solitons, and the other is used as a reference plane wave to determine the phase structure of the solitons. To excite the saddle soliton originated from the X points, the probe beam is reconfigured into three in-phase spots and launched into the lattice without any input tilt [illustrated by three light gray (green online) dots in Fig. 1(a)], with the central spot having a higher intensity. To make sure on-site excitation in the induced index lattice [which has an offset with the intensity pattern as seen in Figs. 1(a) and 1(b)], the three beam spots are aimed at the intensity minima of the lattice beam. The output of the probe beam are monitored with imaging lenses and CCD cameras.

The top panels of Fig. 2 show our typical experimental results, where Fig. 2(a) is the intensity pattern of the observed saddle soliton. From the interference patterns between the soliton beam and the reference plane wave tilted to two different directions [see Figs. 2(b) and 2(c)], we can tell that the soliton possesses uniform and "staggered" phase structure along two orthogonal directions. This kind of phase structure resembles that of the Bloch modes at the first-band X points, as found in our numerical solution of Fig. 1(f). In addition, the k-space spectrum [12] of the soliton also shows that most of its power concentrates at the two X points of the first BZ [Fig. 2(d)]. We emphasize again that, unlike previously observed lattice solitons, this saddle soliton does not arise from single (self-focusing or self-defocusing)
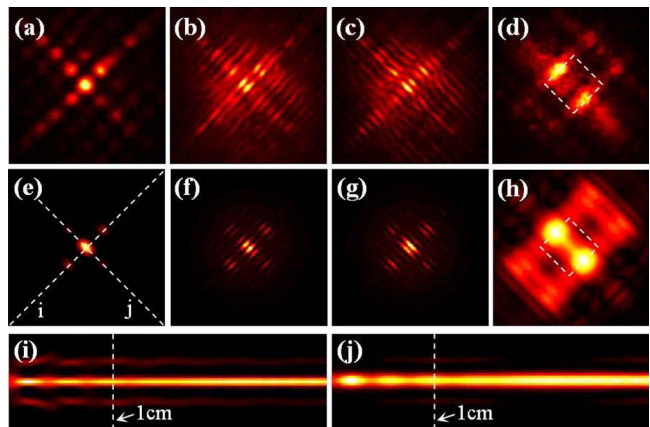

Fig. 2. (Color online) (a)–(d) Experimental and (e)–(j) numerical results of in-gap saddle soliton. The first row shows the (a) intensity pattern; (b), (c) interferograms with a tilted plane wave at two orthogonal directions; and (d) Fourier spectrum of the soliton. The second row shows corresponding numerical results. The third row shows evolution of intensity profiles along dashed lines in (e) for 3 cm propagation of the probe beam.

nonlinearity or single (normal or anomalous) diffraction, but rather it results from a perfect balance between bi-diffraction and hybrid nonlinearity. Since the induced structure depends strongly on the bias condition due to enhanced photorefractive anisotropy, such a balance is realized in the setting illustrated in Fig. 1(a) but can change under other conditions. These results are also corroborated with our numerical simulations [shown in Figs. 2(e) and 2(h)] using parameters close to those from experiment as initial condition. Furthermore, beam propagation to even longer distances (beyond experimental crystal length) shows that the saddle soliton remains stable [Figs. 2(i) and 2(j)].

When the intensity of the lattice-inducing beam is reduced, the bandgap of the 2D ionic lattice becomes narrower or not fully open, as found before for sinusoidal or "backbone" lattices [13]. In this case, quasi-localized saddle soliton solutions can exist with their propagation constant residing even in the Bloch band. A typical example is shown in Fig. 3, which is obtained at $V_0 = 0.5$ while keeping all other parameters unchanged. It can be seen from Fig. 3(a) that the propagation constant resides in the first band rather than in gap, akin to 2D embedded solitons [6]. These modes have similar phase structure and spatial spectrum [Figs. 3(c) and 3(d)] as compared with that of the in-gap saddle solitons [Figs. 1(f) and 1(g)]. However, they are not fully localized in the transverse plane, as they have weak cw tails afar from the center. Thus, these 2D in-band modes are only quasi-localized. If one takes the localized part of these modes as initial condition for propagation, radiation due to leakage to the continuous spectrum is expected. Indeed, long distance propagation [Figs. 3(e) and 3(f)] reveals that they are not stable. Within the experimental crystal length (1 cm), we can still observe them simply at a reduced lattice potential with a single Gaussian beam excitation. The experimental results along with corresponding simulations are depicted in Fig. 4, but the spectrum of the self-trapped state [Fig. 4(d)] extends along the edges of the first BZ instead of condensing at the two X points as in Fig. 2(d), implying their complex constituting mode
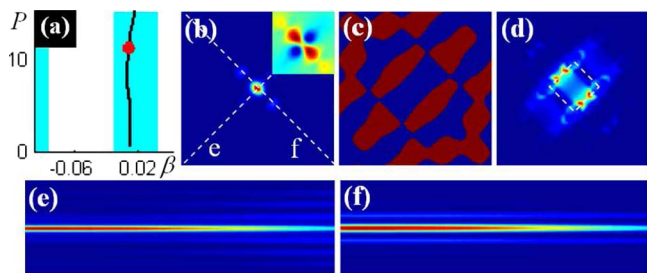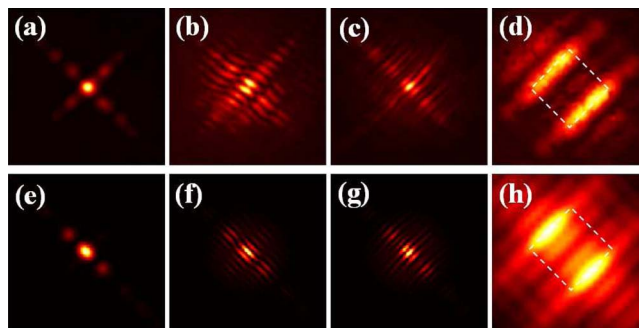

Fig. 4. (Color online) (a)–(d) Experimental and (e)–(h) numerical results of in-band saddle soliton. Other description for Figs. 4(a)–4(h) is the same as that for Figs. 2(a)–2(h).

structures.

In conclusion, we have demonstrated spatial gap solitons due to the perfect balance between hybrid nonlinearity and saddle-shaped diffraction. The existence of saddle solitons may broaden our understanding of soliton phenomena in optics and beyond.

References

1. F. Lederer, G. Stegeman, D. N. Christodoulides, G. Assanto, M. Segev, and Y. Silberberg, Phys. Rep. **463**, 1 (2008).
2. J. Fleischer, M. Segev, N. Efremidis, and D. N. Christodoulides, Nature **422**, 147 (2003).
3. H. Martin, E. Eugenieva, Z. Chen, and D. N. Christodoulides, Phys. Rev. Lett. **92**, 123902 (2004).
4. C. Lou, X. Wang, J. Xu, Z. Chen, and J. Yang, Phys. Rev. Lett. **98**, 213903 (2007).
5. J. Hudock, N. K. Efremidis, and D. N. Christodoulides, Opt. Lett. **29**, 268 (2004).
6. X. Wang, Z. Chen, J. Wang, and J. Yang, Phys. Rev. Lett. **99**, 243901 (2007).
7. J. Yang, B. A. Malomed, and D. J. Kaup, Phys. Rev. Lett. **83**, 1958 (1999).
8. P. Zhang, J. Zhao, C. Lou, X. Tan, Y. Gao, Q. Liu, D. Yang, J. Xu, and Z. Chen, Opt. Express **15**, 536 (2007).
9. Y. Hu, C. Lou, S. Liu, P. Zhang, J. Zhao, J. Xu, and Z. Chen, Opt. Lett. **34**, 1114 (2009).
10. P. Zhang, C. Lou, S. Liu, F. Xiao, J. Zhao, J. Xu, and Z. Chen, Opt. Photonics News **19**(12), 25 (2008).
11. R. Fischer, D. Träger, D. N. Neshev, A. A. Sukhorukov, W. Krolikowski, C. Denz, and Y. S. Kivshar, Phys. Rev. Lett. **96**, 023905 (2006).
12. G. Bartal, O. Cohen, H. Buljan, J. Fleischer, O. Manela, and M. Segev, Phys. Rev. Lett. **94**, 163902 (2005).
13. N. K. Efremidis, J. Hudock, D. N. Christodoulides, J. W. Fleischer, O. Cohen, and M. Segev, Phys. Rev. Lett. **91**, 213906 (2003).

Fig. 3. (Color online) Numerical solutions for quasi-localized in-band saddle soliton at $V_0 = 0.5$. Other description for Figs. 3(a)–3(f) is the same as that for Figs. 1(d)–1(i).